



HAL
open science

Crossing Species Barriers Relies on Structurally Distinct Prion Assemblies and Their Complementation

Angélique Igel-Egalon, Florent Laferrière, Philippe Tixador, Mohammed Moudjou, Laetitia Herzog, Fabienne Reine, Juan Maria Torres, Hubert Laude, Human Rezaei, Vincent Béringue

► **To cite this version:**

Angélique Igel-Egalon, Florent Laferrière, Philippe Tixador, Mohammed Moudjou, Laetitia Herzog, et al.. Crossing Species Barriers Relies on Structurally Distinct Prion Assemblies and Their Complementation. *Molecular Neurobiology*, 2020, 57 (6), pp.2572-2587. 10.1007/s12035-020-01897-3 . hal-03401965

HAL Id: hal-03401965

<https://hal.science/hal-03401965v1>

Submitted on 26 Oct 2021

HAL is a multi-disciplinary open access archive for the deposit and dissemination of scientific research documents, whether they are published or not. The documents may come from teaching and research institutions in France or abroad, or from public or private research centers.

L'archive ouverte pluridisciplinaire **HAL**, est destinée au dépôt et à la diffusion de documents scientifiques de niveau recherche, publiés ou non, émanant des établissements d'enseignement et de recherche français ou étrangers, des laboratoires publics ou privés.

Crossing Species Barriers Relies on Structurally Distinct Prion Assemblies and Their Complementation

Angélique Igel-Egalon^{1¶}, Florent Laferrière^{1¶#}, Philippe Tixador^{1¶∇}, Mohammed Moudjou¹, Laetitia Herzog¹, Fabienne Reine¹, Juan Maria Torres², Hubert Laude¹, Human Rezaei^{1*}, and Vincent Béringue^{1*}

¹VIM, INRAE, Université Paris-Saclay, 78350, Jouy-en-Josas, France,

²Centro de Investigación en Sanidad Animal (CISA-INIA), Valdeolmos, Madrid, Spain

[#]Current address: Institute of Neurodegenerative diseases, CNRS UMR5293, University of Bordeaux, Bordeaux, France

*Corresponding authors:

E-mail: vincent.beringue@inrae.fr (VB), human.rezaei@inrae.fr (HR)

[¶]Equal contributors

Abstract

Background: Prion replication results from the autocatalytic templated assisted conversion of the host-encoded prion protein PrPC into misfolded, polydisperse PrPSc conformers. Structurally distinct PrPSc conformers can give rise to multiple prion strains. Within and between prion strains, the biological activity (replicative efficacy and specific infectivity) of PrPSc assemblies is size dependent and thus reflects an intrinsic structural heterogeneity. The contribution of such PrPSc heterogeneity across species prion adaptation, which is believed to be based on fit adjustment between PrPSc template(s) and host PrPC, has not been explored. To define the structural-to-fitness PrPSc landscape, we measured the relative capacity of size-fractionated PrPSc assemblies from different prion strains to cross mounting species barriers in transgenic mice expressing foreign PrPC. In the absence of a transmission barrier, the relative efficacy of the isolated PrPSc assemblies to induce the disease is like the efficacy observed in the homotypic context. However, in the presence of a transmission barrier, size fractionation overtly delays and even abrogates prion pathogenesis in both the brain and spleen tissues, independently of the infectivity load of the isolated assemblies. Altering by serial dilution PrPSc assembly content of non-fractionated inocula aberrantly reduces their specific infectivity, solely in the presence of a transmission barrier. This suggests that synergy between structurally distinct PrPSc assemblies in the inoculum is requested for crossing the species barrier. Our data support a mechanism whereby overcoming prion species barrier requires complementation between structurally distinct PrPSc assemblies. This work provides key insight into the “quasispecies” concept applied to prions, which would not necessarily rely on prion substrains as constituent but on structural PrPSc heterogeneity within prion population.

Keywords

Prion / species barrier / transgenic mice / quasi-species / sedimentation velocity / assemblies

Background

Mammalian prions are proteinaceous pathogens formed from misfolded assemblies (PrP^{Sc}) of the host-encoded prion protein PrP^C. Prions self-replicate by templating the conversion and polymerization of PrP^C [1]. Prions cause inexorably fatal neurodegenerative diseases such as human Creutzfeldt-Jakob disease (CJD), sheep scrapie, bovine spongiform encephalopathy (BSE) and chronic wasting disease of cervids [2].

The prion strain phenomenon which is due to a structural polymorphism of PrP^{Sc} assemblies is defined by the physiopathological and biochemical characteristics of prion disease within these host species and in experimental models [3-10]. The strain-specified physiopathological differences include duration of disease in the challenged or affected species, vacuolation distribution and pattern of PrP^{Sc} deposition in the brain, tropism for the lymphoid tissue and biochemical properties of PrP^{Sc}, including resistance to denaturation and to proteases [3]. How PrP^{Sc} structural polymorphism causes such distinct phenotypes remains poorly understood.

A broad panel of experimental observations, including by size fractionation supports the existence of structurally different PrP^{Sc} subsets within a given prion strain [11-19]. This intra-strain structural heterogeneity results from the intrinsic and deterministic properties of the prion replication process to generate structurally diverse PrP^{Sc} subsets [20]. Structural diversity is observed at different levels. Size-fractionation studies by sedimentation velocity (SV) indicate that variability in PrP^{Sc} quaternary structure is strain-specific [21,14,15,17,18]. Within a given prion strain, PrP^{Sc} assemblies with differing quaternary structure exhibit markedly different templating and biological activities, which are a hallmark of the existence of structurally distinct PrP^{Sc} subpopulations, as previously discussed [22]. The biological and biochemical consequences of PrP^{Sc} structural heterogeneity during prion replication and propagation are poorly understood.

Maybe one of the most intriguing and unpredictable change in prion replicating environment is the interspecies transmission. In certain host/strain combinations, prions will propagate readily as in an intraspecies transmission. In other host/strain combinations, only a fraction of the exposed animals will develop the disease with variable incubation periods, reflecting a ‘species’ or ‘transmission’ barrier. Attaining full attack rate and minimal incubation periods will require iterative transmissions. At that stage, prions are considered to be adapted to the new host [3]. Two main theoretical models describe the transmission barrier at the molecular level. Both models propose that the species barrier is governed by a misfit between PrP^{Sc} contained in the infecting prion and host PrP^C folding landscape [6,23]. Schematically, the first model called ‘deformed templating’ considers, by analogy with the *in vivo* adaptation of synthetic prions (i.e., obtained by inoculation of amyloid fibrils of recombinant PrP [24]) that PrP^C will progressively adopt, -due to its specific conformational dynamic-, the “quasi-right” conformation to be selected during the templating process [23]. As a consequence, a switch to a new strain structural determinant can occur, which combines structural information from the inoculated PrP^{Sc} assemblies with the folding landscape of the new host PrP^C [25-29]. A major limitation of this model resides in the assumption that all PrP^{Sc} assemblies are structurally equivalent, despite experimental counter-evidence. The second model called ‘conformational selection’ considers the existence of structurally distinct PrP^{Sc} subsets within a strain or isolate (“cloud”), the species adaptation resulting from the selection of the best replicator [6]. The two models are not mutually exclusive. They at least have the merit to highlight the role of structural diversity of PrP^C and/or PrP^{Sc} in prion adaptation and evolution.

Here, we aim at defining the contribution of PrP^{Sc} (quaternary) structure polydispersity to across species prion fitness. We compare the relative capacity of size-fractionated PrP^{Sc} assemblies to propagate in transgenic mice expressing homotypic versus heterotypic PrP^C, used as proxy of mounting species barriers (one with prion ‘mutation’). We show that fractionating PrP^{Sc}

assemblies strengthens existing species barrier, to a degree of magnitude independent of their infectivity load. Crossing species barriers may thus require coexistence of heterogeneous PrP^{Sc} quaternary structure in the inoculum. We strengthen this hypothesis by showing that altering, by serial dilution, PrP^{Sc} assemblies content overtly reduces the specific infectivity from non-fractionated inocula during cross-species transmission events. Our data support a mechanism whereby overcoming prion species barrier requires complementation between structurally distinct PrP^{Sc} subsets within the inoculum, refining the current prion adaptation models.

Methods

Transgenic mouse lines

The transgenic mouse lines expressing ovine, hamster and bovine PrP have been previously described [30-33]. The bovine PrP tg540 [30] and tg110 [31] lines showed equivalent susceptibilities to classical BSE prions [30].

Prion sources

LA19K, LA21K *fast* and 127S scrapie prions are cloned prion strains. They have been obtained by serial transmission and subsequent biological cloning by limiting dilutions of classical field scrapie isolates to tg338 transgenic mice expressing the VRQ allele of ovine PrP [33,34,18]. Pooled tg338 mouse brain homogenates (20% wt/vol. in 5% glucose) were used for centrifugation analyses, as indicated.

L-type BSE is a natural bovine isolate (designated BASE by the authors [35]). The transmission properties of this isolate in tgBov mice (tg540 line) and tgOv mice have been previously described [26]. The same brain material from the same isolate was transmitted to tgBov line (tg110) line by intracerebral route by using 20 µl of a 10% (wt/vol. in 5% glucose) brain homogenate.

Fractionation by sedimentation velocity

The sedimentation velocity procedure has been previously and comprehensively described [13,15,18,20]. Briefly, detergent-solubilized brain homogenates were loaded atop a continuous 10–25% iodixanol gradient (Optiprep, Axys-shield). The gradients were centrifuged at 285 000 g for 45 min in a swinging-bucket SW-55 rotor using an Optima LE-80K ultracentrifuge (Beckman Coulter). Gradients were then manually segregated into 30 equal fractions of 165 µl from the bottom using a peristaltic pump. Fractions were aliquoted for immunoblot and bioassays. Gradient linearity was verified by refractometry. To avoid any cross-contamination, each piece of equipment was thoroughly decontaminated with 5 M NaOH followed by several rinses in deionised water after each gradient collection.

Bioassays

Fractions were diluted extemporarily in 5% glucose (1:5) in a class II microbiological cabinet according to a strict protocol to avoid any cross-contamination. Individually identified 6- to 10-week-old mice were inoculated intracerebrally with 20 µl of the solution, using a 27-gauge disposable syringe needle inserted into the right parietal lobe. At terminal stage of disease or at end-life, mice were euthanized and analyzed for proteinase K (PK) resistant PrP^{Sc} (PrP^{res}) content in brains and spleens tissues (as indicated), using the Bio-Rad TsSeE detection kit [26] before immunoblotting, as described below.

Endpoint titration

For titration purposes, groups of indicator mice were inoculated intracerebrally (20 µl) with serial ten-fold dilutions of the indicated brain homogenates. Animals inoculated with the initial dose at 10% (w/v) solution were assigned an infectious dose of 0. The mice were monitored daily, euthanized at terminal stage, and analyzed as above for PrP^{res} content. The survival times of tgBov or tgHa reporter mice were measured for each tenfold dilution tested and the relative infectious dose / survival time relationship was reported, when available. It allows translating

survival times of the inoculated fractions in infectious dose (i.e., equivalent to that found in brain homogenate dilutions) as estimate of infectivity.

Immunoblots

Aliquots of the collected fractions (40 μ l) were treated with a final concentration of 50 μ g/ml PK (1 hour, 37°C). Samples were then mixed in Laemmli buffer and denatured at 100°C for 5 min. The equivalent of 10 μ l of the fractions was run on 12% Bis-Tris Criterion gels (Bio-Rad, Marne la Vallée, France) and analyzed by immunoblots, using the Sha31 anti-PrP antibody (human PrP epitope at residues 145 to 152 [36]). Immunoreactivity was visualized by chemiluminescence (GE Healthcare). The amount of PrP present per fraction and the PrP^{Sc} glycoforms ratios were determined with the GeneTools software after acquisition of chemiluminescent signals with a GeneGnome digital imager (Syngene, Frederick, Maryland, United States).

Histoblots

For histoblotting procedure, brains were rapidly removed from euthanized mice and frozen on dry ice. Cryosections were cut at 8–10 μ m, transferred onto Superfrost slides and kept at -20°C until use. Histoblot analyses were performed on 3 brains per experiment, using the 12F10 anti-PrP antibody (human PrP epitope at residues 145 to 160 [37]) or 3F4 anti-PrP antibody (human PrP epitope at residues 109 to 112 [38]), as indicated.

Results

Modelling prion species barrier in transgenic animals

To determine the potential role of size-fractionated PrP^{Sc} subpopulations in prion adaptation and evolution, we included in the present study three well-characterized, cloned ovine prion strains termed LA19K, LA21K *fast* and 127S. We also included atypical L-BSE prions in the study, because of their mutability on cross-species transmission [26].

We transmitted size-fractionated-PrP^{Sc} assemblies from LA19K, LA21K *fast/127S* and L-BSE prions to transgenic mice expressing bovine, hamster and ovine PrP, respectively. These mouse lines were chosen according to the transmission barrier observed with non-fractionated material, as examined by gold-standard criteria [39-41], including disease attack rate on primary passage, reduction of incubation durations (ID) on serial passaging, and establishment of prion strain properties. After two or three passages in the heterotypic PrP context, we performed the same analyses on back-passage to mice expressing the parental host PrP^C. For the sake of clarity, these data are shown as [Additional file 1, Fig. 1-4](#). However, to provide a straightforward estimator of the stringency of the species barrier, we used the reduction factor between the mean ID on first to second passage in the heterotypic PrP context and on retrotransmission ([Fig. 1a](#), [41]). A magnitude of 1 signifies prion straight adaptation.

As transgenic model of prion transmission without species barrier, we passed LA19K scrapie prions from ovine PrP mice (tgOv) to bovine PrP mice (tg540 [42] or tg110 [31] line; tgBov). Iterative transmission and retrotransmission of LA19K prions occurred in these lines without drastic evolution of time to disease onset, PrP^{Sc} biochemical properties and PrP^{Sc} distribution in brain and spleen tissues ([additional File 1, supplementary Fig. 1](#)). The magnitude of the transmission barrier was ~1 ([Fig. 1a](#)).

As model of prion transmission with species barrier and ‘mutation’, we passed cattle L-BSE prions onto tgOv mice ([additional File 1, supplementary Fig. 2](#) and [43]). L-BSE prions adaptation to tgOv mice required iterative passages, resulting in a transmission barrier magnitude value of ~3 ([Fig. 1a](#)). This adaptation was accompanied by a “mutation” of L-BSE prions into classical-like BSE (C-BSE) prions [43]. However, L-BSE prions were readily reisolated on back-passage to tgBov mice, without any significant transmission barrier, as based on the mean ID and regain of L-type phenotypic identity ([Fig. 1a, additional File 1, supplementary Fig. 2a-c](#)).

As models of prion transmission with marked species barrier, we passed LA21K *fast* and 127S scrapie prions onto hamster PrP mice (tg7 line [32]; tgHa). These two prion strains can adapt to tgHa mice and be reisolated without strain identity change in tgOv mice ([additional File 1, supplementary Fig. 3-4](#)). Yet, at each of these crossings, iterative passages were necessary to attain minimal IDs, resulting in transmission barrier magnitudes of ~3.5 (tgOv → tgHa) and ~6-fold (tgHa → tgOv) ([Fig. 1a](#)). Such lengthy readaptation differs from other retrotransmission studies termed ‘traceback’ in which readaptation occurred readily [44,41,45]. In these studies, backpassaging was performed after a single passage in the new host. It is likely that ability to readily retrotransmit is lost after serial passages in the new host (as we did here), due to improved adaptation.

Impact of size-fractionation on prion pathogenesis in mice expressing heterotypic PrP

We used a previously developed SV protocol to separate different populations of PrP^{Sc} assemblies according to their quaternary structure [13,15,18,20]. It allowed us to show that LA19K, LA21K *fast* and 127S strains markedly differ according to the specific infectivity of their respective PrP^{Sc} subpopulations in the homotypic PrP transmission conditions. For LA21K *fast* and 127S strains, a discrete population of small oligomers (<pentamers) exhibit the highest specific infectivity values. For LA19K, the highest specific infectivity values are associated with larger-size oligomers (>40 PrP-mers) [22]. Here, we solubilized and SV-fractionated brain homogenates from tgOv mice containing LA19K prions, LA21K *fast* or 127S prions and from cattle containing L-BSE prions. We inoculated the fractions by intracerebral route to transgenic mice expressing heterotypic PrP^C to determine the specific transmission property of each fraction. ([Fig. 1b](#)). As controls, we transmitted some fractions to transgenic mice expressing homotypic PrP and confirmed our previous results ([18]; see below).

In the absence of any apparent PrP transmission barrier, as determined for LA19K inoculated to tgBov mice, the infectivity sedimentograms in the homotypic and heterotypic passage

conditions, tended to superimpose, in terms of distribution and infectivity values amongst the fractions (Fig. 2a). Each LA19K isolated PrP^{Sc} assembly thus exhibited quasi-equivalent specific infectivity in both transmission contexts. The strain-specified PrP^{res} electrophoretic profile and pattern of cerebral PrP^{res} deposition [32] were conserved amongst the tgBov mice inoculated with the different fractions or with unfractionated LA19K brain material (Fig. 2b, Fig. 3a), suggesting phenotypic invariance of the isolated LA19K assemblies on heterotypic transmission.

In the presence of a marked species barrier, as determined for LA21K *fast* and 127S inoculated to tgHa mice, SV-fractionation had a strong negative impact. None of the mice inoculated with the fractions from three independent gradients developed any neurological symptoms up to end-life. Only 3 out of the 221 tested mice (i.e., 1%) accumulated PrP^{res} in the brain. These 3 mice were inoculated with fractions 10 and 13 from one LA21K *fast* gradient (Fig. 4, Table 1). Notably, none of the tgHa mice inoculated with the PrP^{Sc} assemblies exhibiting the highest specific infectivity values from fractions 1-2 accumulated any detectable PrP^{res} (n=43, Table 1).

These results were confirmed by a second passage with individual or pooled (by 2) tgHa brains, covering the entire LA21K *fast* gradient. All the secondary transmissions with PrP^{res}-negative brains were negative (neurological signs and PrP^{res}; Table 2), indicating absence of a subclinical disease [46,45] and/or of infectious, PK-sensitive PrP^{Sc} species [47,16] in the non-responder mice. Oppositely, serial transmissions from PrP^{res}-positive brains led to isolation of prions with strains properties identical to those obtained on adaptation of unfractionated LA21K *fast* prions to tgHa mice (Table 2, Fig. 3b, Fig. 4b, Additional file 1, supplementary Fig. 3b).

To discard the possibility that the loss of tgHa-transmissibility of the isolated PrP^{Sc} was due to an insufficient infectivity load, we first estimated the infectivity levels of the top and middle fractions of one LA21K *fast* gradient in the homotypic PrP context. Fractions 2 and 12 induced

disease in tgOv mice in 68 ± 3 days (5/5) and 82 ± 1 days (5/5), respectively (Fig. 4a), meaning, according to LA21K *fast* dose/response curve (Fig. 4a, Table 3), that their infectivity levels were equivalent to $10^{-1.2}$ and $10^{-3.2}$ dilutions of LA21K *fast* brain material, respectively. These values were in the range of the previously established mean (\pm SEM) relative infectious dose contained in LA21K *fast* most infectious upper fractions and middle fractions (from seven independent bioassays: top fractions: mean: $10^{-1.36}$ ($10^{-1.08}$ to $10^{-1.64}$); middle fractions: between $10^{-2.9}$ and $10^{-4.65}$ depending on the middle fractions). Next, we examined whether such infectivity load was enough to induce disease in the heterotypic PrP context. To achieve this, we established a dose/response curve of LA21K *fast* in tgHa mice. We inoculated by intracerebral route serial tenfold dilutions of a LA21K *fast* tgOv-brain to reporter tgHa mice. The limiting dilution value of LA21K *fast* prions in tgHa mice was surprisingly low (see below), establishing at 10^{-2} (Table 3). Nevertheless, this value was below the infectivity value of the upper fractions of the LA21K *fast* gradient. Those were thus sufficiently infectious *per se* to induce or transmit disease, at least partly in tgHa mice. This was not observed in 3 independent experiments with $n=43$ inoculated mice (Table 2). Almost counterintuitively, the sole fractions eliciting asymptomatic replication in a very low number of mice had infectivity values below the limiting dilution. This suggests a stochastic transmission process and lends support to the view that infection is possible at doses below the limiting dilution [48].

Together, these observations indicate that PrP^{Sc} subassemblies segregation by SV-fractionation alters their replication efficiency in the PrP transmission barrier context, independently of their infectivity load. This suggests that synergetic interactions between PrP^{Sc} subsets are necessary to cross a transmission barrier.

Dilution of LA21K *fast* prion-infected brain homogenate strengthens the transmission barrier

To further explore a synergetic effect between different PrP^{Sc} subsets, we turned to dilution experiments as a relevant method to explore the contribution of each PrP^{Sc} subtype. LA21K *fast* prions are composed of at least two structurally PrP^{Sc} subsets in different proportion, each with distinct specific infectivity (for review [22]). Over a certain dilution factor, the minor population will be quasi-eliminated from the inoculum leading to explore the effect of the major species. The dilution approaches should also allow dissociating biochemical complex(es) between different PrP^{Sc} subsets due to equilibrium displacement toward dissociation [13].

We thus further analyzed the titration of LA21K *fast* prions in tgHa mice. Neat brain homogenate (20 μ L 10%) containing LA21K *fast* prions induced disease in all inoculated tgHa mice with a mean ID of 153 days (Table 3; Additional file 1, supplementary Fig. 3a). At the 10⁻¹ dilution, the mean ID increased to 181 days with a 100% attack rate. Strikingly, the limiting dilution value resulting in positive transmission established at the 10⁻² dilution, with 2 out of 6 tgHa mice developing the disease at 192 and 230 days (Table 3). In homotypic transmission, LA21K *fast* limiting dilution value established at 10⁻⁷ (Table 3). There was thus a considerable 10⁵-fold reduction of this value in the heterotypic PrP transmission context. For comparison, in the absence of a transmission barrier, as for LA19K prions in tgBov mice, there was no significant variations in the limiting dilution value between the homotypic and heterotypic contexts (Table 3).

The inefficacy of LA21K *fast* diluted material to infect tgHa mice appeared further discrepant when considering the fold increase between the IDs at the lowest and at the limiting dilution. There was a 1.37-fold increase for LA21K *fast* in tgHa mice (from 153 to 211 days, Table 3, Fig. 5a) whereas the mean \pm SD fold increase value observed in all the titrations we performed so far in our laboratory in homotypic conditions, including in tgHa mice, was statistically

higher, establishing at 2.17 ± 0.32 ($p < 0.05$, One-sample z test; Fig. 5a). Applying this value to LA21K *fast* titration in tgHa mice would result in a theoretical limiting dilution value at $\sim 10^{-5}$ and a ~ 330 days ID (Fig. 5b).

Collectively, these data suggest that the dilution leads to the quasi elimination of at least one compound and/or the dissociation of a complex mandatory for the efficacy of the heterotypic transmission. They thus consolidate our SV-based observations.

PrP^C level and/or tissue environment imposes the species barrier stringency

We finally examined the issue of the transmission of SV-fractionated L-BSE prions to tgOv mice. None of the L-BSE SV-fractions inoculated to tgOv mice induced a clinical disease at full attack rate (Table 4). A slightly higher proportion of mice euthanized at end-life accumulated PrP^{res} in the brain, suggesting possibility of subclinical infection. Fractions 8 to 14 were the most efficient to induce clinical or subclinical disease (Fig. 6a, Table 4). The top and bottom fractions induced a clinical or subclinical disease erratically, suggesting unfavorable transmission conditions (Fig. 6a, Table 4). Isolated L-BSE assemblies had therefore altered transmission capacities in the heterotypic PrP transmission context, as observed with LA21K *fast* and 127S prions.

The western blot profile on primary passage (Fig. 6b) and the strain phenotype obtained on 2nd passage with PrP^{res}-positive mouse brains (Table 5, Fig. 3c) indicated that C-BSE like prions has emerged from all positive transmissions.

Previously, we reported that lymphotropic prions replicated easier in the spleen than in the brain in both homotypic and heterotypic PrP context, despite 20-fold lowered PrP^C levels [27,49]. This makes bioassays based on prion detection in the mouse spleen a highly sensitive method to detect low dose of lymphotropic prions [49]. We thus examined further the capacity of SV-fractionated L-BSE prions to propagate in the heterotypic PrP context by examining tgOv spleens for PrP^{res} content after inoculation with the different fractions. Of the 49 tgOv spleens

analyzed, only 3 (6%) accumulated low levels of PrP^{res} (Table 4). Of the 13 mice for which both the brains and spleens were analyzed for PrP^{res} content and the brain was positive (notably fractions 10-12 with the highest attack rates), only 3 had also positive spleens (23%). For comparison, all the spleens analyzed after inoculation of unfractionated L-type prions were strongly PrP^{res}-positive from the first passage onward (Table 4, [50]).

Strikingly, prion replication in the spleen was still altered on secondary passage of SV-fractionated L-BSE assemblies. While all the spleens analyzed (n=15) were PrP^{res}-positive, the levels of accumulation were still reduced by ~4-fold as compared to those observed on serial transmission of unfractionated material (Fig. 7a-b). It may be noted that in homotypic transmissions, fractionating brain material had no significant influence on spleen colonization by prions, regarding the number of positive spleens and PrP^{res} accumulation levels (Fig. 7b), indicating that, alone, the size of the infectious particles or PrP^{Sc} subpopulation segregation were not causal. Therefore, we can conclude that size fractionation impairs L-BSE replication in the spleen to an extent that is higher than in the brain.

Discussion

As conventional pathogens, prions are subject to adaptation and evolution. The concept of molecular quasispecies, as defined by Eigen in 1979 [51], has been applied to prions [6,52] to reconcile the structural diversity of prion assemblies (i.e. prion structural landscape) to the preferential selection, based on the ‘best replicator’ selection concept, of certain subassemblies during prion adaptation to new host or to a new environment/replicating conditions [27,53]. To refine this ‘best replicator’ hypothesis [54], we tested the capacity of isolated PrP^{Sc} subassemblies within a given prion strain to adapt to a new host. We show here with PrP transgenic mouse models inoculated with both field-derived and biologically cloned prions, that cross-species prion transmission does not strictly involve the selection of an existing

subpopulation of optimized PrP^{Sc} assemblies. Rather, our observations suggest that the key determinant is a synergy between structurally distinct PrP^{Sc} subassemblies.

There was a positive correlation between the magnitude of the transmission barrier and the difficulty for SV-individualized PrP^{Sc} assemblies to transmit the disease in the heterotypic PrP conditions. LA19K scrapie prions propagated without apparent transmission barrier in bovine PrP mice, whether SV-fractionated or not. In marked contrast, L-BSE prions fractionation significantly delayed priogenesis in the brain and even more negatively in the spleen of the challenged tgOv mice. Fractionated LA21K *fast* scrapie prions replicated asymptotically in a very small proportion of tgHa mice and fractionated 127S prions failed to propagate in these mice. As shown previously and also demonstrated here, LA21K *fast* and 127S scrapie prion strains are composed of at least two structurally distinct PrP^{Sc} subpopulations according to their specific infectivity values (Fig. 4a and for review [22]). The loss of transmissibility of separately taken PrP^{Sc} assemblies to tgHa mice cannot be attributed to a global decrease of infectivity levels due to the solubilization/fractionation method as we previously reported that the cumulated infectivity of the SV fractions did not differ significantly from that present in the loaded material [18]. Further, for LA21K *fast*, the relative infectivity titer of the top ‘most infectious’ fractions was sufficiently high to induce disease in tgHa. Another hypothesis is that SV-fractionation segregates potential co-factors from the PrP^{Sc} assemblies [55-57]. We would need to assume that such segregation affects PrP^{Sc} assemblies fitness solely in situations of heterotypic transmission with existing barriers, in both neural and lymphoid tissues. Further, in the case of LA21K *fast* and 127S prions, fractionation impacted the transmission capacities of all assemblies, irrespectively of their size/specific activity. We would expect such co-factors being present in one of these fractions and help, particularly in the top ones if of lipid nature. Overall, this co-factor hypothesis is extremely unlikely. The fact that PrP^{Sc} assemblies segregation affects prion heterospecies transmission suggests a synergy between PrP^{Sc}

subassemblies to overcome the species barrier. This hypothesis implicates an unprecedented notion of complementation between structurally distinct prion assemblies.

While the molecular mechanisms of such synergy between different PrP^{Sc} subsets remain to be elucidated, some simple biochemical considerations can bring basements on the biochemistry of the process. It implicates interactions between structurally distinct PrP^{Sc} subsets to create a new structural information absent in each individual PrP^{Sc} population and leading to heterologous PrP^C integration. During the early stage of prion replication, we showed that two sets of structurally distinct PrP^{Sc} assemblies are generated, in fractions 1-5 and 10-18 [20]. These sets are defined by their elementary subunit [13] as suPrP^A and suPrP^B, respectively. During the early step of prion replication, suPrP^A and suPrP^B form a suPrP^A:suPrP^B heterocomplex involved in a secondary autocatalytic templating process generating *de novo* the formation of suPrP^B, in a PrP^C-dependent manner [20]. The synergetic effect between different PrP^{Sc} subsets can reside in the formation of this complex, making therefore this secondary templating process a pivot of prion adaptation to a new host. In the heterotypic PrP transmission context, the suPrP^A:suPrP^B complex (likely present in the inoculum) may incorporate heterologous PrP^C, due to structural constraints on the templating interface generated by the heteroassembly formation [58]. This would lead to the formation of a *de novo* suPrP^{B*} formed by the heterologous PrP^C with a new templating interface different from the inoculum suPrP^B (Fig. 8). This first event would be a limiting step of the adaptation process. The entrance of suPrP^{B*} in the autocatalytic cycle makes its formation highly cooperative. Based on these assumptions, if the stability of the complex is high enough (i.e., low dissociation constant), the reconstitution of the initial composition by mixing different PrP^{Sc} subsets should allow recovering the transmission efficiency. This approach has been unsuccessful with LA21K *fast* prions. This fail could be due to the weakness of the suPrP^A:suPrP^B complex, as previously observed [20]. Indeed, size exclusion chromatography analysis of the 127S suPrP^A:suPrP^B

complex revealed that this last is highly labile and can be observed only in conditions where the concentration of suPrP^A and suPrP^B were high.

The existence of a complex such as suPrP^A:suPrP^B within the inoculum is further supported by the striking observation that endpoint dilutions aberrantly impaired LA21K *fast* prions transfer to tgHa mice (1000-fold decreased efficacy); the dilution steps would make certain PrP^{Sc} subpopulations disappearing given their ratio/amount and/or induce the dissociation of an existing complex [13,59]. While cross-species transmission of prions has rarely been done at high dilution, it may be noted that comparing the limiting dilution values of MM1 sporadic CJD prions (homozygous for Met at codon 129) in transgenic mice expressing human PrP with either Met or Val at codon 129 resulted in 10³-fold decrease [60], a negative impact quantitatively comparable to our observations.

If the synergy between structurally different PrP^{Sc} subsets involves the formation of a suPrP^A:suPrP^B heterocomplex and the PrP^C-dependent secondary templating pathway, the magnitude of the species barrier would thus depend both on the strength of the heterocomplex and on the amount of heterotypic PrP^C which defines the rate of the secondary templating and its cooperativity aspect [20]. Such prominent role of PrP^C is experimentally supported by the observation that L-BSE prions adaptation is more impaired in tg338 mouse spleen than brain, despite a potentially favored local environment for heterotypic conversion as prion species barrier is lower in the spleen than in the brain [27]. The lower concentrations of PrP^C [34] in the spleen [27] and/or the different structure (including the post-translational modifications) may impact the secondary templating pathway and its autocatalytic nature.

Whether complementation between heteroassemblies is specific of cross-species transmission with existing species barrier or occurred in all interspecies transmissions remains to be determined. In the absence of a transmission barrier, as for LA19K in bovine PrP mice, there was no effect of SV-fractionation on the disease pathogenesis in terms of attack rate, time to

disease onset, infectivity sedimentogram and strain phenotype. If complementation is necessary, it is currently not visible by standard prion phenotyping.

Here, we used scrapie laboratory strains that are found in ovine and caprine hosts [34,61,62,33,63] and L-BSE, a natural cattle isolate. Our transgenic-based approach allowed studying and modeling the molecular aspects of the species barrier regarding PrP conversion. Since deconstructing prion inoculum increases the strength of the species barrier, this phenomenon is likely to impact prion capacity to infect new hosts in the context of natural, peripheral infection, where only a fraction of the inoculum passes the digestive barrier.

Conclusion

Together, our data would expand the prion quasispecies concept to an ensemble of macromolecular assemblies, -not necessarily associated to different substrains-, that complement each other to adapt tissue-specific selection pressure and extend prion host range. Such ‘epistatic’ behavior may provide new fundamental principles for understanding prion distinctive properties to transfer between species [64] and can explain the relative inability of recombinant PrP to generate high-titer prions [65], unless submitted to intense mechanisms of polymerization/fragmentation which may generate aggregate polydispersity and/or a larger portfolio of conformations [57] for complementation.

List of Abbreviations

Bov: bovine

BSE: bovine spongiform encephalopathy

CJD; Creutzfeldt-Jakob disease

Ha: hamster

Ov: ovine

PrP: prion protein

PK: proteinase K

PrP^{res}: proteinase K resistant PrP^{Sc}

PrP^{Sc}: pathological/abnormal form of the prion protein

suPrP: PrP elementary brick

SV: sedimentation velocity

tg: transgenic

Declarations

Ethics approval

All the experiments involving animals were carried out in strict accordance with EU directive 2010/63 and were approved by INRA local ethics committee (Comethea; permit numbers 12-034 and 15-056).

Consent for publication

Not applicable.

Availability of data and material

All data supporting our findings are presented in the main paper and additional files.

Competing interests

The authors declare no competing financial interests.

Funding

This work was funded by the Fondation pour la Recherche Médicale (Equipe FRM DEQ20150331689), the European Research Council (ERC Starting Grant SKIPPERAD, number 306321), and the Ile de France region (DIM MALINF).

Acknowledgments

We thank the staff of Infectiology of fishes and rodent facilities (INRAE, Jouy-en-Josas, France; doi:10.15454/1.5572427140471238E12) for animal care, Dr Benjamin Dehay for critical reading of the manuscript.

Author's contribution

Conceptualization, AIE, FL, PT, MM, HL, HR, and VB; Data curation and Analysis, AIE, FL, PT, MM, LH, FR, JMT, HL, HR, and VB; Resources, HL, JMT, HR and VB; Writing – Original Draft, AIE, HR, and VB; Writing – Review and Editing, AIE, HR, and VB; Visualization, AIE, HR and VB; Supervision, VB; Funding Acquisition, HR and VB; All authors read and approved the final manuscript.

References

1. Prusiner SB (1982) Novel proteinaceous infectious particles cause scrapie. *Science* 216 (4542):136-144
2. Collinge J (2001) Prion diseases of humans and animals: their causes and molecular basis. *Annu Rev Neurosci* 24:519-550
3. Beringue V, Vilotte JL, Laude H (2008) Prion agent diversity and species barrier. *Vet Res* 39 (4):47. doi:10.1051/vetres:2008024
v08241 [pii]
4. Bessen RA, Marsh RF (1992) Identification of two biologically distinct strains of transmissible mink encephalopathy in hamsters. *J Gen Virol* 73 (Pt 2):329-334
5. Bruce ME (2003) TSE strain variation. *Br Med Bull* 66:99-108
6. Collinge J, Clarke AR (2007) A general model of prion strains and their pathogenicity. *Science* 318 (5852):930-936

7. Sim VL, Caughey B (2009) Ultrastructures and strain comparison of under-glycosylated scrapie prion fibrils. *Neurobiol Aging* 30 (12):2031-2042. doi:10.1016/j.neurobiolaging.2008.02.016
8. Spassov S, Beekes M, Naumann D (2006) Structural differences between TSEs strains investigated by FT-IR spectroscopy. *Biochim Biophys Acta* 1760 (7):1138-1149. doi:S0304-4165(06)00042-0 [pii]
10.1016/j.bbagen.2006.02.018
9. Telling GC, Parchi P, DeArmond SJ, Cortelli P, Montagna P, Gabizon R, Mastrianni J, Lugaresi E, Gambetti P, Prusiner SB (1996) Evidence for the conformation of the pathologic isoform of the prion protein enciphering and propagating prion diversity. *Science* 274 (5295):2079-2082
10. Weissmann C, Li J, Mahal SP, Browning S (2011) Prions on the move. *EMBO Rep* 12 (11):1109-1117. doi:embor2011192 [pii]
10.1038/embor.2011.192
11. Bett C, Joshi-Barr S, Lucero M, Trejo M, Liberski P, Kelly JW, Masliah E, Sigurdson CJ (2012) Biochemical properties of highly neuroinvasive prion strains. *PLoS Pathog* 8 (2):e1002522. doi:10.1371/journal.ppat.1002522
PPATHOGENS-D-11-02044 [pii]
12. Bett C, Lawrence J, Kurt TD, Orru C, Aguilar-Calvo P, Kincaid AE, Surewicz WK, Caughey B, Wu C, Sigurdson CJ (2017) Enhanced neuroinvasion by smaller, soluble prions. *Acta Neuropathol Commun* 5 (1):32. doi:10.1186/s40478-017-0430-z
13. Igel-Egalon A, Moudjou M, Martin D, Busley A, Knapple T, Herzog L, Reine F, Lepejova N, Richard CA, Beringue V, Rezaei H (2017) Reversible unfolding of infectious prion

assemblies reveals the existence of an oligomeric elementary brick. *PLoS Pathog* 13 (9):e1006557. doi:10.1371/journal.ppat.1006557

14. Kim C, Haldiman T, Surewicz K, Cohen Y, Chen W, Blevins J, Sy MS, Cohen M, Kong Q, Telling GC, Surewicz WK, Safar JG (2012) Small Protease Sensitive Oligomers of PrP(Sc) in Distinct Human Prions Determine Conversion Rate of PrP(C). *PLoS Pathog* 8 (8):e1002835. doi:10.1371/journal.ppat.1002835

PPATHOGENS-D-12-00720 [pii]

15. Laferriere F, Tixador P, Moudjou M, Chapuis J, Sibille P, Herzog L, Reine F, Jaumain E, Laude H, Rezaei H, Beringue V (2013) Quaternary structure of pathological prion protein as a determining factor of strain-specific prion replication dynamics. *PLoS Pathog* 9 (10):e1003702. doi:10.1371/journal.ppat.1003702

PPATHOGENS-D-13-00529 [pii]

16. Sajnani G, Silva CJ, Ramos A, Pastrana MA, Onisko BC, Erickson ML, Antaki EM, Dynin I, Vazquez-Fernandez E, Sigurdson CJ, Carter JM, Requena JR (2012) PK-sensitive PrP is infectious and shares basic structural features with PK-resistant PrP. *PLoS Pathog* 8 (3):e1002547. doi:10.1371/journal.ppat.1002547

PPATHOGENS-D-11-01621 [pii]

17. Silveira JR, Raymond GJ, Hughson AG, Race RE, Sim VL, Hayes SF, Caughey B (2005) The most infectious prion protein particles. *Nature* 437 (7056):257-261. doi:nature03989 [pii]

10.1038/nature03989

18. Tixador P, Herzog L, Reine F, Jaumain E, Chapuis J, Le Dur A, Laude H, Beringue V (2010) The physical relationship between infectivity and prion protein aggregates is strain-dependent. *PLoS Pathog* 6 (4):e1000859. doi:10.1371/journal.ppat.1000859

19. Tzaban S, Friedlander G, Schonberger O, Horonchik L, Yedidia Y, Shaked G, Gabizon R, Taraboulos A (2002) Protease-sensitive scrapie prion protein in aggregates of heterogeneous sizes. *Biochemistry* 41 (42):12868-12875. doi:bi025958g [pii]
20. Igel-Egalon A, Laferriere F, Moudjou M, Bohl J, Mezache M, Knapple T, Herzog L, Reine F, Jas-Duval C, Doumic M, Rezaei H, Beringue V (2019) Early stage prion assembly involves two subpopulations with different quaternary structures and a secondary templating pathway. *Commun Biol* 2:363. doi:10.1038/s42003-019-0608-y
21. Haldiman T, Kim C, Cohen Y, Chen W, Blevins J, Qing L, Cohen ML, Langeveld J, Telling GC, Kong Q, Safar JG (2013) Co-existence of distinct prion types enables conformational evolution of human PrP^{Sc} by competitive selection. *J Biol Chem* 288 (41):29846-29861. doi:10.1074/jbc.M113.500108
22. Igel-Egalon A, Bohl J, Moudjou M, Herzog L, Reine F, Rezaei H, Beringue V (2019) Heterogeneity and Architecture of Pathological Prion Protein Assemblies: Time to Revisit the Molecular Basis of the Prion Replication Process? *Viruses* 11 (5). doi:10.3390/v11050429
23. Makarava N, Baskakov IV (2013) The evolution of transmissible prions: the role of deformed templating. *PLoS Pathog* 9 (12):e1003759. doi:10.1371/journal.ppat.1003759
24. Baskakov IV (2014) The many shades of prion strain adaptation. *Prion* 8 (2). doi:10.4161/pri.27836
25. Asante EA, Linehan JM, Desbruslais M, Joiner S, Gowland I, Wood AL, Welch J, Hill AF, Lloyd SE, Wadsworth JD, Collinge J (2002) BSE prions propagate as either variant CJD-like or sporadic CJD-like prion strains in transgenic mice expressing human prion protein. *EMBO J* 21 (23):6358-6366
26. Beringue V, Andreoletti V, LE DUR A, Essalmani R, Vilotte JL, Lacroux C, Reine F, Herzog L, Biacabè A-G, Baron T, Caramelli M, Casalone C, Laude H (2007) A bovine prion

- acquires an epidemic bovine spongiform encephalopathy strain-like phenotype on interspecies transmission. *Journal of Neuroscience* 27 (26):6965-6971. doi:10.1523/jneurosci.0693-07.2007
27. Beringue V, Herzog L, Jaumain E, Reine F, Sibille P, Le Dur A, Vilotte JL, Laude H (2012) Facilitated cross-species transmission of prions in extraneural tissue. *Science* 335 (6067):472-475. doi:10.1126/science.1215659
- 335/6067/472 [pii]
28. Chapuis J, Moudjou M, Reine F, Herzog L, Jaumain E, Chapuis C, Quadrio I, Boulliat J, Perret-Liaudet A, Dron M, Laude H, Rezaei H, Beringue V (2016) Emergence of two prion subtypes in ovine PrP transgenic mice infected with human MM2-cortical Creutzfeldt-Jakob disease prions. *Acta neuropathologica communications* 4 (1):2-15. doi:10.1186/s40478-016-0284-9
29. Scott MR, Groth D, Tatzelt J, Torchia M, Tremblay P, DeArmond SJ, Prusiner SB (1997) Propagation of prion strains through specific conformers of the prion protein. *J Virol* 71 (12):9032-9044
30. Beringue V, Bencsik A, LE DUR A, Reine F, Lan Lai T, Chenais N, Tilly G, BiacabÈ A-G, Baron T, Vilotte JL, Laude H (2006) Isolation from cattle of a prion strain distinct from that causing bovine spongiform encephalopathy. *Plos Pathogens* 2 (10):956-963. doi:10.1371/journal.ppat.0020112
31. Castilla J, Gutierrez Adan A, Brun A, Pintado B, Ramirez MA, Parra B, Doyle D, Rogers M, Salguero FJ, Sanchez C, Sanchez-Vizcaino JM, Torres JM (2003) Early detection of PrPres in BSE-infected bovine PrP transgenic mice. *Arch Virol* 148 (4):677-691. doi:10.1007/s00705-002-0958-4
32. Hecker R, Taraboulos A, Scott M, Pan KM, Yang SL, Torchia M, Jendroska K, DeArmond SJ, Prusiner SB (1992) Replication of distinct scrapie prion isolates is region specific in brains of transgenic mice and hamsters. *Genes Dev* 6 (7):1213-1228

33. Langevin C, Andreoletti O, Le Dur A, Laude H, Beringue V (2011) Marked influence of the route of infection on prion strain apparent phenotype in a scrapie transgenic mouse model. *Neurobiol Dis* 41 (1):219-225. doi:S0969-9961(10)00311-6 [pii]
10.1016/j.nbd.2010.09.010
34. Le Dur A, Lai TL, Stinnakre MG, Laisne A, Chenais N, Rakotobe S, Passet B, Reine F, Soulier S, Herzog L, Tilly G, Rezaei H, Beringue V, Vilotte JL, Laude H (2017) Divergent prion strain evolution driven by PrPC expression level in transgenic mice. *Nat Commun* 8:14170. doi:10.1038/ncomms14170
35. Casalone C, Zanusso G, Acutis P, Ferrari S, Capucci L, Tagliavini F, Monaco S, Caramelli M (2004) Identification of a second bovine amyloidotic spongiform encephalopathy: molecular similarities with sporadic Creutzfeldt-Jakob disease. *Proc Natl Acad Sci U S A* 101 (9):3065-3070. doi:10.1073/pnas.0305777101
36. Feraudet C, Morel N, Simon S, Volland H, Frobert Y, Creminon C, Vilette D, Lehmann S, Grassi J (2005) Screening of 145 anti-PrP monoclonal antibodies for their capacity to inhibit PrPSc replication in infected cells. *J Biol Chem* 280 (12):11247-11258. doi:10.1074/jbc.M407006200
37. Krasemann S, Groschup MH, Harmeyer S, Hunsmann G, Bodemer W (1996) Generation of monoclonal antibodies against human prion proteins in PrP0/0 mice. *Mol Med* 2 (6):725-734
38. Kascsak RJ, Rubenstein R, Merz PA, Tonna-DeMasi M, Fersko R, Carp RI, Wisniewski HM, Diringer H (1987) Mouse polyclonal and monoclonal antibody to scrapie-associated fibril proteins. *J Virol* 61 (12):3688-3693
39. Kimberlin RH, Walker CA (1978) Evidence that the transmission of one source of scrapie agent to hamsters involves separation of agent strains from a mixture. *J Gen Virol* 39 (3):487-496. doi:10.1099/0022-1317-39-3-487

40. Kimberlin RH, Walker CA, Fraser H (1989) The genomic identity of different strains of mouse scrapie is expressed in hamsters and preserved on reisolation in mice. *J Gen Virol* 70 (Pt 8):2017-2025. doi:10.1099/0022-1317-70-8-2017
41. Nonno R, Di Bari MA, Cardone F, Vaccari G, Fazzi P, Dell'Omo G, Cartoni C, Ingrosso L, Boyle A, Galeno R, Sbriccoli M, Lipp HP, Bruce M, Pocchiari M, Agrimi U (2006) Efficient transmission and characterization of Creutzfeldt-Jakob disease strains in bank voles. *PLoS Pathog* 2 (2):e12. doi:10.1371/journal.ppat.0020012
42. Beringue V, Bencsik A, Le Dur A, Reine F, Lai TL, Chenais N, Tilly G, Biacabe AG, Baron T, Vilotte JL, Laude H (2006) Isolation from cattle of a prion strain distinct from that causing bovine spongiform encephalopathy. *PLoS Pathog* 2 (10):e112. doi:06-PLPA-RA-0212R3 [pii] 10.1371/journal.ppat.0020112
43. Beringue V, Andreoletti O, Le Dur A, Essalmani R, Vilotte JL, Lacroux C, Reine F, Herzog L, Biacabe AG, Baron T, Caramelli M, Casalone C, Laude H (2007) A bovine prion acquires an epidemic bovine spongiform encephalopathy strain-like phenotype on interspecies transmission. *J Neurosci* 27 (26):6965-6971. doi:10.1523/JNEUROSCI.0693-07.2007
44. Kobayashi A, Asano M, Mohri S, Kitamoto T (2009) A traceback phenomenon can reveal the origin of prion infection. *Neuropathology* 29 (5):619-624. doi:10.1111/j.1440-1789.2008.00973.x
45. Race R, Chesebro B (1998) Scrapie infectivity found in resistant species. *Nature* 392 (6678):770. doi:10.1038/33834
46. Hill AF, Joiner S, Linehan J, Desbruslais M, Lantos PL, Collinge J (2000) Species-barrier-independent prion replication in apparently resistant species. *Proc Natl Acad Sci U S A* 97 (18):10248-10253. doi:10.1073/pnas.97.18.10248

47. Cronier S, Gros N, Tattum MH, Jackson GS, Clarke AR, Collinge J, Wadsworth JD (2008) Detection and characterization of proteinase K-sensitive disease-related prion protein with thermolysin. *Biochem J* 416 (2):297-305. doi:10.1042/BJ20081235
48. Fryer HR, McLean AR (2011) There is no safe dose of prions. *PLoS One* 6 (8):e23664. doi:10.1371/journal.pone.0023664
49. Halliez S, Reine F, Herzog L, Jaumain E, Haik S, Rezaei H, Vilotte JL, Laude H, Beringue V (2014) Accelerated, spleen-based titration of variant Creutzfeldt-Jakob disease infectivity in transgenic mice expressing human prion protein with sensitivity comparable to that of survival time bioassay. *J Virol* 88 (15):8678-8686. doi:10.1128/JVI.01118-14
50. Al-Dybiat I, Moudjou M, Martin D, Reine F, Herzog L, Truchet S, Berthon P, Laude H, Rezaei H, Andreoletti O, Beringue V, Sibille P (2019) Prion strain-dependent tropism is maintained between spleen and granuloma and relies on lymphofollicular structures. *Sci Rep* 9 (1):14656. doi:10.1038/s41598-019-51084-1
51. Eigen M, Schuster P (1977) The hypercycle. A principle of natural self-organization. Part A: Emergence of the hypercycle. *Naturwissenschaften* 64 (11):541-565
52. Shorter J (2010) Emergence and natural selection of drug-resistant prions. *Mol Biosyst* 6 (7):1115-1130. doi:10.1039/c004550k
53. Li J, Browning S, Mahal SP, Oelschlegel AM, Weissmann C (2010) Darwinian evolution of prions in cell culture. *Science* 327 (5967):869-872. doi:10.1126/science.1183218
54. Nee S (2016) The evolutionary ecology of molecular replicators. *R Soc Open Sci* 3 (8):160235. doi:10.1098/rsos.160235
55. Deleault NR, Piro JR, Walsh DJ, Wang F, Ma J, Geoghegan JC, Supattapone S (2012) Isolation of phosphatidylethanolamine as a solitary cofactor for prion formation in the absence of nucleic acids. *Proc Natl Acad Sci U S A* 109 (22):8546-8551. doi:10.1073/pnas.1204498109

56. Deleault NR, Walsh DJ, Piro JR, Wang F, Wang X, Ma J, Rees JR, Supattapone S (2012) Cofactor molecules maintain infectious conformation and restrict strain properties in purified prions. *Proc Natl Acad Sci U S A* 109 (28):E1938-1946. doi:10.1073/pnas.1206999109
57. Wang F, Wang X, Yuan CG, Ma J (2010) Generating a prion with bacterially expressed recombinant prion protein. *Science* 327 (5969):1132-1135. doi:10.1126/science.1183748
58. Spagnolli G, Rigoli M, Orioli S, Sevillano AM, Faccioli P, Wille H, Biasini E, Requena JR (2019) Full atomistic model of prion structure and conversion. *PLoS Pathog* 15 (7):e1007864. doi:10.1371/journal.ppat.1007864
59. Masel J, Jansen VA (2001) The measured level of prion infectivity varies in a predictable way according to the aggregation state of the infectious agent. *Biochim Biophys Acta* 1535 (2):164-173. doi:10.1016/s0925-4439(00)00095-8
60. Huor A, Douet JY, Lacroux C, Lugan S, Tillier C, Aron N, Cassard H, Arnold M, Torres JM, Ironside JW, Andreoletti O (2017) Infectivity in bone marrow from sporadic CJD patients. *J Pathol*. doi:10.1002/path.4954
61. Vilotte JL, Soulier S, Essalmani R, Stinnakre MG, Vaiman D, Lepourry L, Da Silva JC, Besnard N, Dawson M, Buschmann A, Groschup M, Petit S, Madelaine MF, Rakatobe S, Le Dur A, Vilette D, Laude H (2001) Markedly increased susceptibility to natural sheep scrapie of transgenic mice expressing ovine prp. *J Virol* 75 (13):5977-5984. doi:10.1128/JVI.75.13.5977-5984.2001
62. Foster JD, Dickinson AG (1988) The unusual properties of CH1641, a sheep-passaged isolate of scrapie. *Vet Rec* 123 (1):5-8
63. Nonno R, Marin-Moreno A, Carlos Espinosa J, Fast C, Van Keulen L, Spiropoulos J, Lantier I, Andreoletti O, Pirisinu L, Di Bari MA, Aguilar-Calvo P, Sklaviadis T, Pappasavva-Stylianou P, Acutis PL, Acin C, Bossers A, Jacobs JG, Vaccari G, D'Agostino C, Chiappini B, Lantier F, Groschup MH, Agrimi U, Maria Torres J, Langeveld JPM (2020) Characterization

of goat prions demonstrates geographical variation of scrapie strains in Europe and reveals the composite nature of prion strains. *Sci Rep* 10 (1):19. doi:10.1038/s41598-019-57005-6

64. Aguzzi A, Rajendran L (2009) The transcellular spread of cytosolic amyloids, prions, and prionoids. *Neuron* 64 (6):783-790. doi:10.1016/j.neuron.2009.12.016

65. Schmidt C, Fizet J, Properzi F, Batchelor M, Sandberg MK, Edgeworth JA, Afran L, Ho S, Badhan A, Klier S, Linehan JM, Brandner S, Hosszu LL, Tattum MH, Jat P, Clarke AR, Klohn PC, Wadsworth JD, Jackson GS, Collinge J (2015) A systematic investigation of production of synthetic prions from recombinant prion protein. *Open Biol* 5 (12):150165. doi:10.1098/rsob.150165

Figures

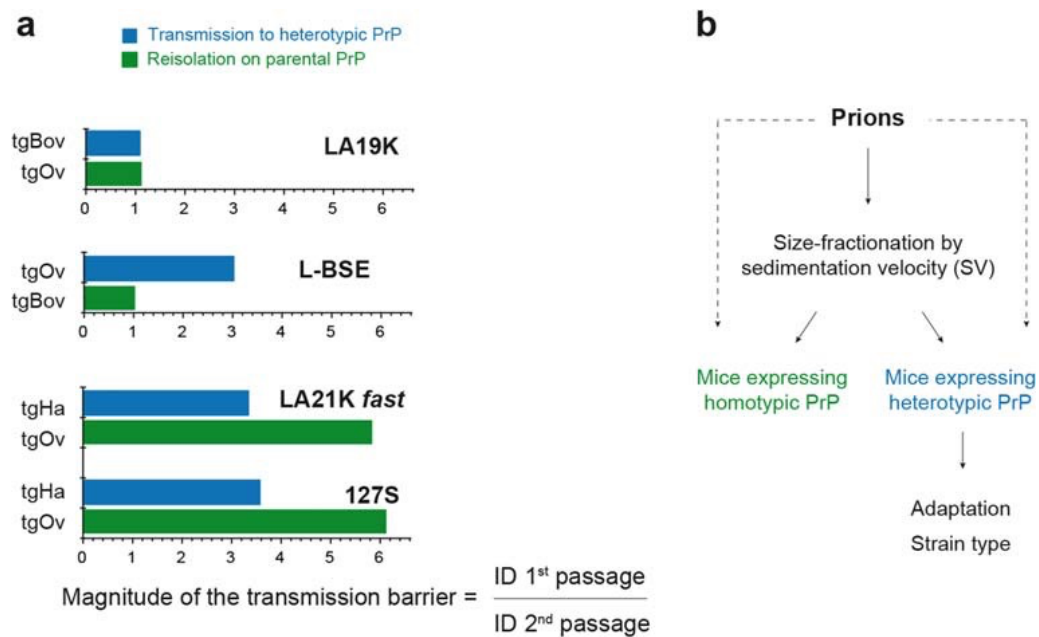


Figure 1. Magnitude of the species barrier on transmission of scrapie prions (LA19K, LA21K *fast*, 127S) and cattle prions (L-BSE) to transgenic mice expressing heterotypic PrP

(a) Scrapie LA19K, LA21K *fast*, 127S prions and cattle L-BSE prions were transmitted iteratively to mice expressing bovine PrP (tgBov), hamster PP (tgHa) and ovine PrP (tgOv), respectively, before reisolation in transgenic mice expressing the parental PrP ([Additional file 1](#)). The magnitude of the transmission barrier in transgenic mice expressing heterotypic PrP (blue color) and on reisolation in transgenic mice expressing the parental PrP (green color) was calculated as the ratio of the mean incubation durations (ID) on first to second passage in the

new host PrP and on reisolation in mice expressing the parental PrP. A magnitude of 1 signifies prion straight adaptation.

(b) Overview of the bioassays made with PrP^{Sc} assemblies fractionated by sedimentation velocity.

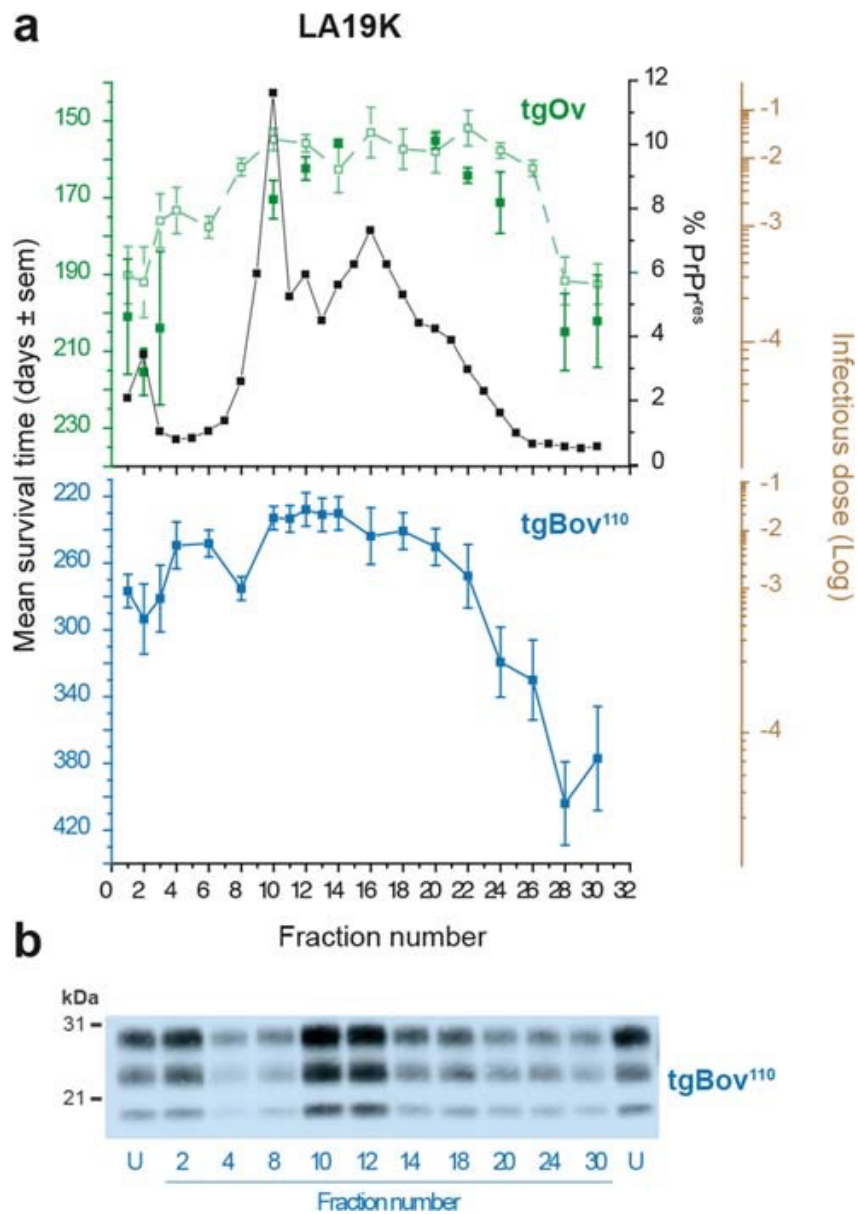


Figure 2. Unaltered capacity of SV-fractionated PrP^{Sc} assemblies to propagate onto a new host PrP sequence in the absence of a transmission barrier

(a) SV profiles of PrP^{res} (black line) and infectivity in the homotypic PrP (green line) and heterotypic PrP (blue line) transmission context. Brain homogenates from tgOv mice inoculated with LA19K prions were solubilized before fractionation by SV. The collected fractions were analyzed for PrP^{res} content by immunoblot and for infectivity by an incubation time bioassay in tgOv and tgBov mice (tg110 line). In the homotypic context, plain and dotted symbols/lines refer to this study and to previous reports [18], respectively. The right logarithmic brown scale provides the LA19K-specific reciprocal relation between survival time in tgOv and tgBov mice

and infectious dose, as established by limiting dilution titration (as from [Table 3](#) and [18]).

Animals inoculated with 10% infectious brain material are assigned an infectious dose of 0.

(b) PrP^{res} electrophoretic profiles in the brains of tgBov mice inoculated with size-fractionated LA19K-tgOv PrP^{Sc} assemblies. The profile obtained with unfractionated (U) material is shown for comparison.

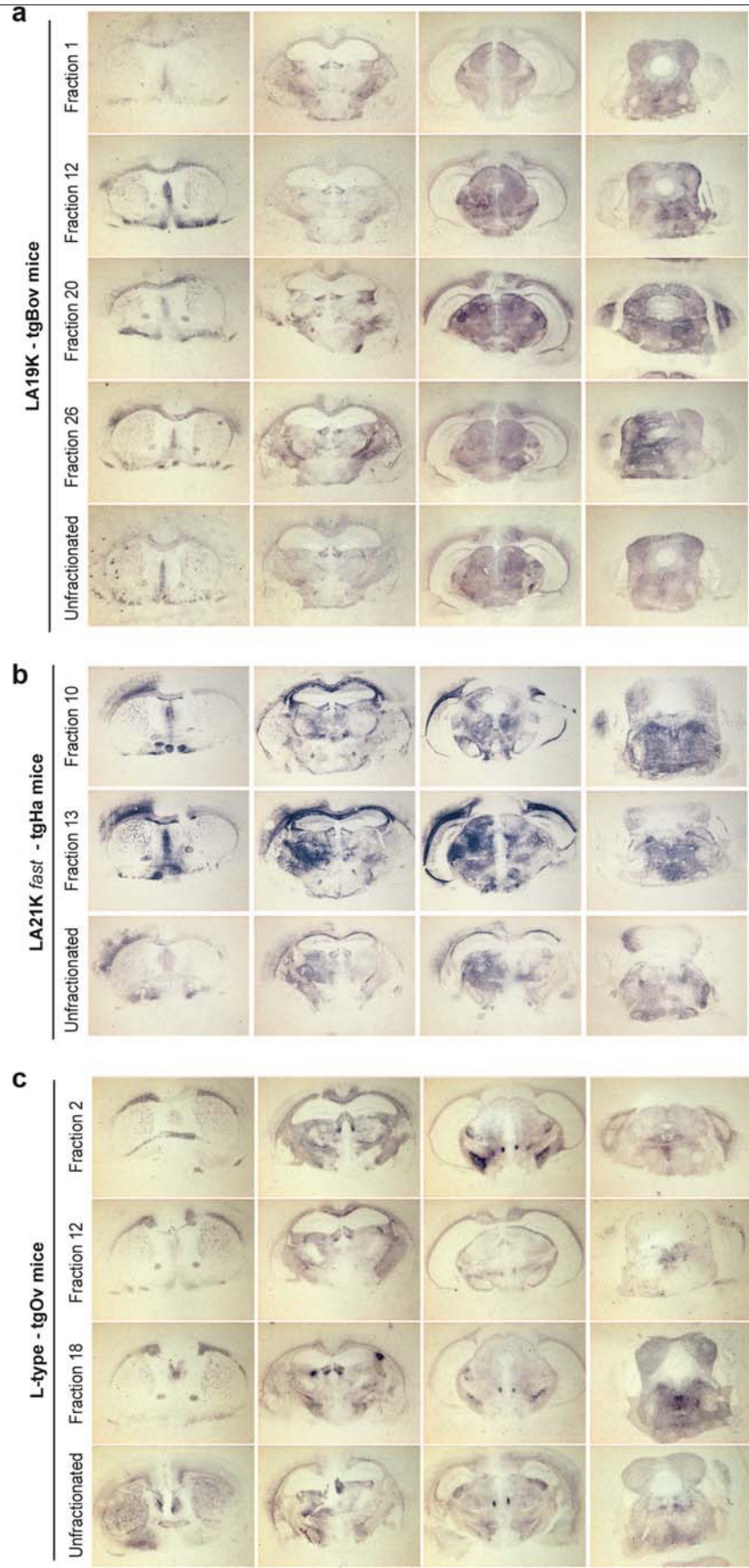


Figure 3. Neuroanatomical pattern of PrP^{res} deposition in tgBov, tgHa and tgOv mice inoculated with fractionated or unfractionated LA19K, LA21K *fast* and L-BSE prions

tgBov (tg110 line (a)), tgHa mice (b) and tgOv (c) mice were inoculated with fractionated or unfractionated LA19K, LA21K *fast* and L-type BSE prions, respectively. Representative histoblots of antero-posterior coronal brain sections (1st passage for LA19K (12F10 antibody), 2nd passage for LA21K *fast* (3F4 antibody), 2nd passage for L-BSE, (12F10 antibody)) at the level of the septum, hippocampus, midbrain and brainstem (from left to right) are shown.

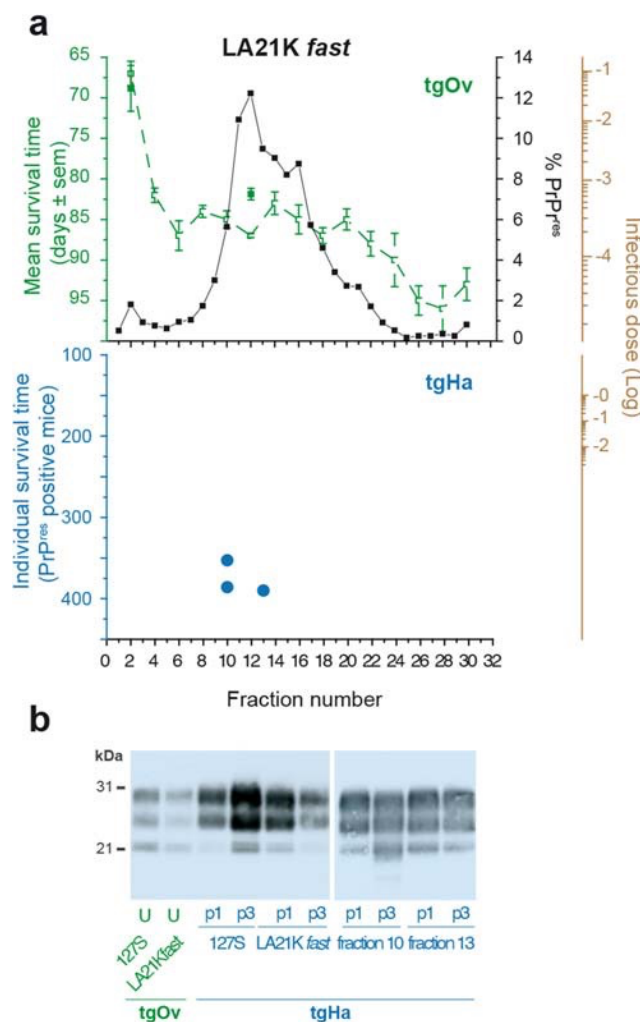


Figure 4. Altered capacity of size-fractionated PrP^{Sc} assemblies to propagate onto a new host PrP sequence in the presence of a marked transmission barrier

(a) SV profiles of PrP^{res} (black line) and infectivity in the homotypic PrP (green line) and heterotypic PrP (blue dots) transmission context. Brain homogenates from tgOv mice inoculated with LA21K *fast* prions were solubilized before fractionation by SV. The collected fractions were analyzed for PrP^{res} content by immunoblot and for infectivity by an incubation time bioassay in tgOv and tgHa mice. In the homotypic context, plain and dotted symbols/lines refer to this study and to previous reports [18], respectively. Because of the reduced penetrance of the disease in tgHa mice, the mean individual ID of the PrP^{res} positive mice are shown as blue dots. The right logarithmic brown scale provides the LA21K *fast*-specific reciprocal relation between survival time in tgHa and tgOv mice and infectious dose, as established by

limiting dilution titration (as from [Table 3](#) and [18]). Animals inoculated with 10% infectious brain material are assigned an infectious dose of 0.

(b) PrP^{res} electrophoretic profiles in the brains of tgHa mice inoculated with size-fractionated LA21K *fast* prions at the 1st (p1) and 3rd (p3) passage. The profiles obtained with unfractionated (U) LA21K *fast* and 127S material in tgOv and tgHa mice are shown for comparison.

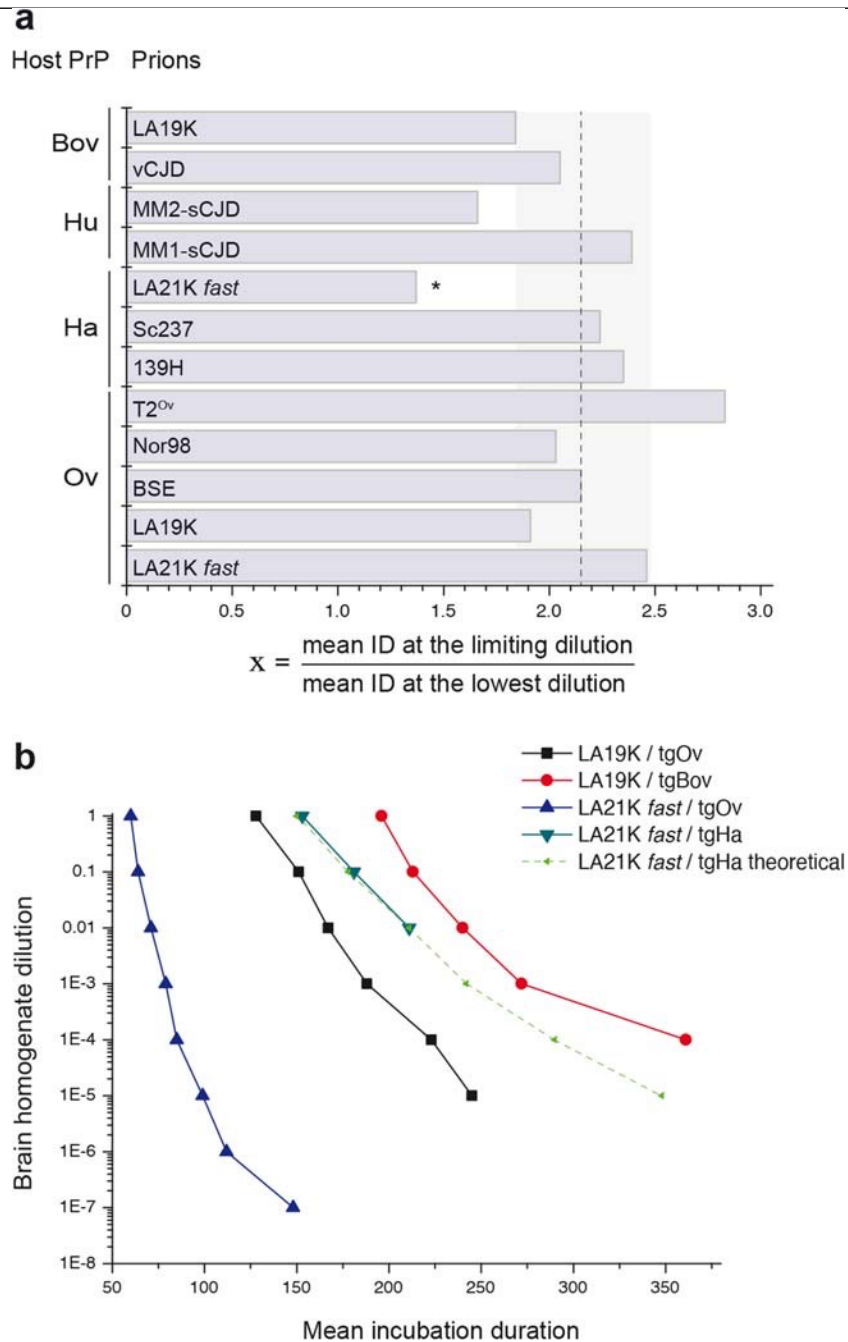


Figure 5. Aberrant titration of LA21K *fast* prion in hamster PrP mice as compared to other prion titrations in PrP transgenic mice

(a) Fold increase (x) between the mean IDs at the lowest and at the limiting dilution during prion titrations. The prions titrated and the reporter mice are indicated on the graph. The mean \pm SD value observed for all but the LA21K *fast* \rightarrow tgHa titrations established at 2.17 \pm 0.32

(mean \pm SD, dotted vertical line: mean; shadow square: SD). The 1.37-fold increase for LA21K *fast* in tgHa mice is significantly lower (* $p < 0.05$, One-sample z test).

(b) Titration curve of LA19K prions in tgOv and tgBov mice as compared to that of LA21K *fast* in tgOv and tgHa mice. The theoretical curve of LA21K *fast* prions in tgHa mice is the result of the 2.17-fold increase in the IDs at the lowest and at the limiting dilution.

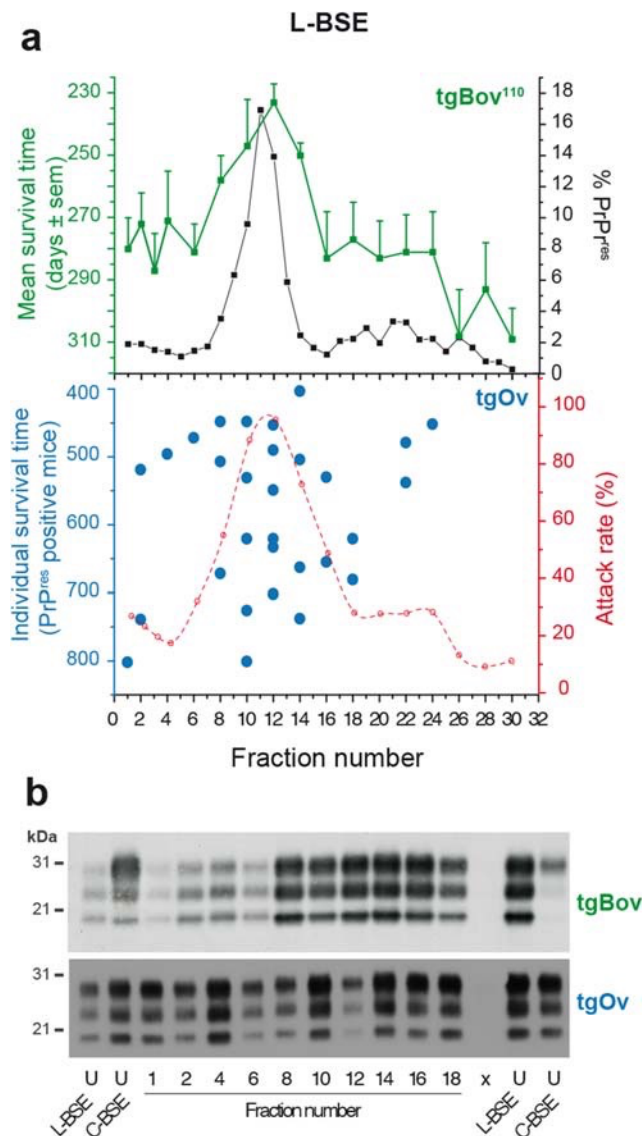


Figure 6. Capacity of size-fractionated PrP^{Sc} assemblies to propagate onto a new host PrP sequence in the presence of a significant transmission barrier with mutation

(a) SV profiles of PrP^{res} (black line) and infectivity in the homotypic PrP (green line) and heterotypic PrP (blue dots) transmission context. Brain homogenates from cattle infected with L-BSE prions were solubilized before fractionation by SV. The collected fractions were analyzed for PrP^{res} content by immunoblot and for infectivity by an incubation time bioassay in tgBov and tgOv mice. The subclinical/clinical disease attack rate in tgOv mice is presented on the right red graph. Because of the reduced penetrance of the disease in tgOv mice, the mean individual ID of the PrP^{res} positive mice are shown as blue dots.

(b) PrP^{res} electrophoretic profiles in the brains of tgOv and tgBov mice inoculated with size-fractionated L-BSE PrP^{Sc} assemblies. The profiles obtained with unfractionated (U) material from L-BSE or classical BSE (C-BSE) are shown for comparison.

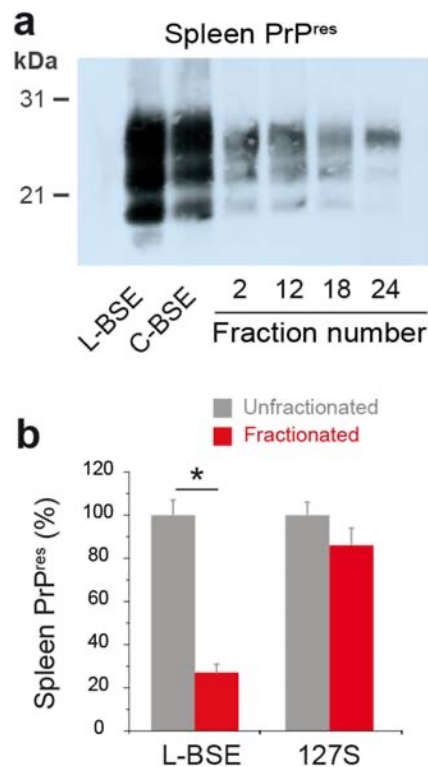


Figure 7. Capacity of size-fractionated L-BSE prions to colonize the spleens of mice expressing homotypic or heterotypic PrP^C

(a) PrP^{res} detection in the spleens of tgOv mice inoculated with unfractionated L-BSE or C-BSE prions (primary passage) or with fractionated L-BSE prions (second passage, fractions used for passaging are indicated).

(b) PrP^{res} accumulation levels in the spleens of tgOv mice inoculated with unfractionated (2nd passage) or SV-fractionated L-BSE ((all fractions combined), 2nd passage) prions as compared to unfractionated or SV-fractionated 127S prions. (* $p < 0.05$, Mann-Whitney test).

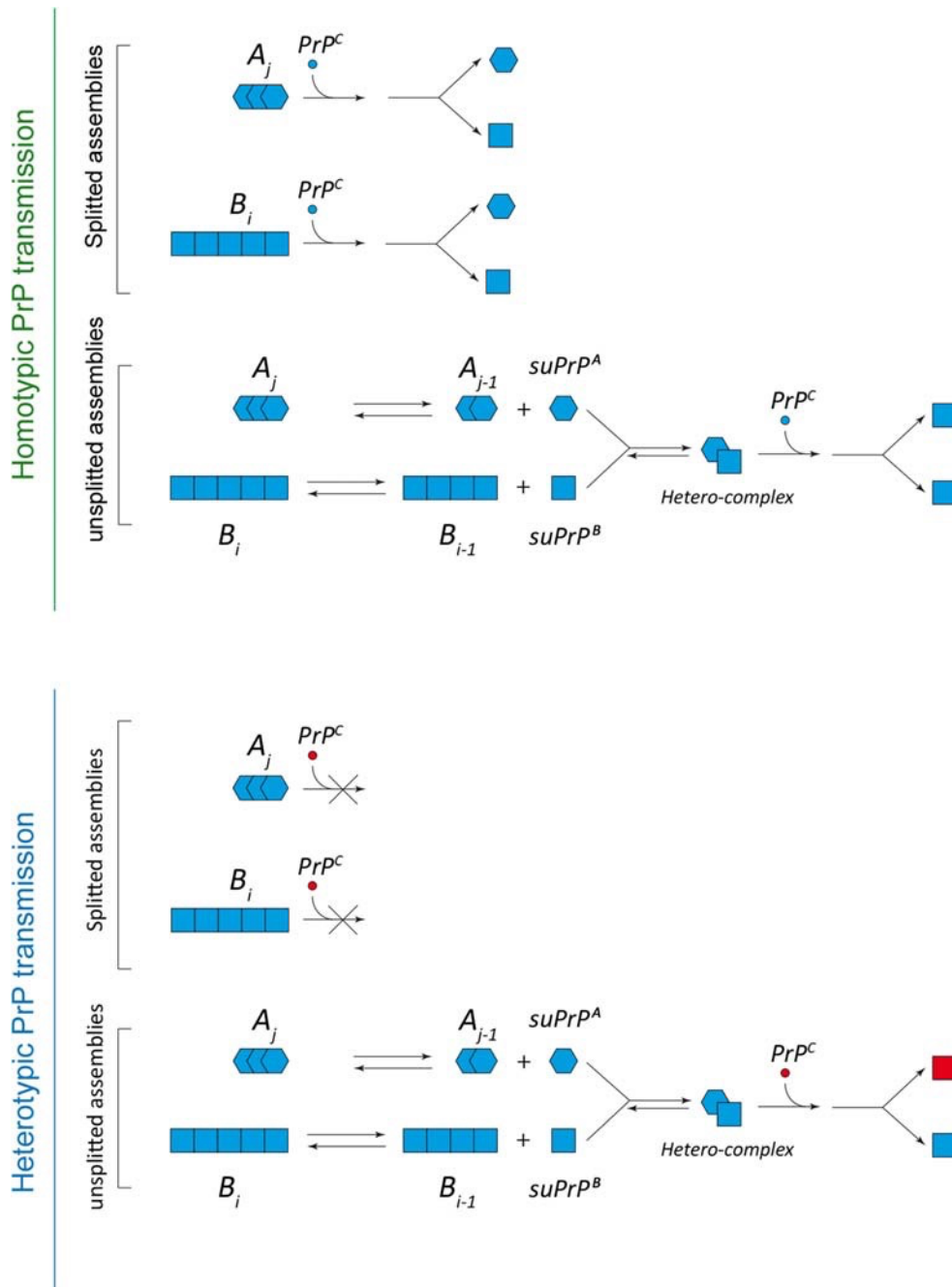


Figure 8. The formation of heterocomplex between structurally distinct PrP^{Sc} subsets may drive the conversion of heterologous PrP^C by a secondary templating pathway process

(a) In the homotypic PrP transmission context, prion replication involves two templating pathways: a primary templating pathway where structurally distinct PrP^{Sc} subsets, taken individually (A_j and B_i), are able to perpetuate the strain information and a PrP^C-dependent

autocatalytic secondary templating pathway contributing to structural diversification, which requires the formation of a heterocomplex between the elementary subunits of two structurally distinct sets of PrP^{Sc} assemblies (suPrP^A and suPrP^B) [20].

(b) This autocatalytic secondary templating pathway could drive the incorporation of heterologous PrP^C during the species barrier passage, leading to *de novo* generation of suPrP^B (in red) more prone to replicate/propagate in the new host. PrP^{Sc} assemblies segregation or dilution could drastically affect the formation of the suPrP^A:suPrP^B complex, compromising this secondary templating pathway.

Tables

Table 1. Summary of the transmission of SV-fractionated LA21K *fast* and 127S prions to hamster PrP mice

Fractions	LA21K <i>fast</i>				127S							
	Total attack rate	Clinical signs	PrP ^{res} 1	Survival ² (days ± SEM)	Total attack rate	Clinical signs	PrP ^{res} 1	Survival ² (days ± SEM)	Total attack rate	Clinical signs	PrP ^{res} 1	Survival ² (days ± SEM)
1	0/12	0/12	0/12	399-627	0/5	0/5	0/5	384-631	0/6	0/6	0/6	365-552
2	0/13	0/13	0/13	520-692	0/6	0/6	0/6	318-576	0/5	0/5	0/5	341-496
3	0/5	0/5	0/5	389-651	0/6	0/6	0/6	401-636	0/5	0/5	0/5	405-538
4	0/5	0/5	0/5	507-647	0/6	0/6	0/6	384-535	0/6	0/6	0/6	317-506
6	0/6	0/6	0/6	386-780								
8	0/6	0/6	0/6	375-713								
10	2/6	0/6	2/6	353; 386	0/6	0/6	0/6	461-531	0/6	0/6	0/6	331-510
11	0/5	0/5	0/5	536-937	0/6	0/6	0/6	378-517				
12	0/11	0/11	0/11	347-687	0/6	0/6	0/6	322-426	0/6	0/6	0/6	382-587
13	1/6	0/6	1/6	394								
14	0/6	0/6	0/6	556-720	0/6	0/6	0/6	344-629	0/6	0/6	0/6	481-631
15	0/6	0/6	0/6	323-854								
16	0/6	0/6	0/6	614-710								
18	0/6	0/6	0/6	325-839								
20	0/6	0/6	0/6	406-877								
22	0/6	0/6	0/6	371-751								
24	0/5	0/5	0/5	543-927								
26	0/6	0/6	0/6	413-602								
28	0/6	0/6	0/6	345-749								
30	0/6	0/6	0/6	383-665								
U³	8/8	8/8	8/8	157 ± 6					8/8	8/8	8/8	168 ± 7

¹Positive for brain PrP^{res} by immunoblotting or histoblotting.

²For mice negative for disease clinical signs and for PrP^{res} accumulation, only the range of survival time is given.

³U: unfractionated material ([Additional File 1, supplementary Fig. 3](#)).

Table 2. Serial passage of SV-fractionated LA21K *fast* prions in hamster PrP mice

Fractions (mouse no. ¹)	LA21K <i>fast</i>											
	2 nd passage				3 rd passage				4 th passage			
	Total attack rate	Clinical signs	PrP ^{res} 2	Survival ³ (days ± SEM)	Total attack rate	Clinical signs	PrP ^{res} 2	Survival ³ (days ± SEM)	Total attack rate	Clinical signs	PrP ^{res} 2	Survival ³ (days ± SEM)
1 (no. 2+3)	0/6	0/6	0/6	382-524								
2 (no.4+7)	0/6	0/6	0/6	301-605								
10 (no.1+2)	6/6	6/6	6/6	54 ± 1	6/6	6/6	6/6	50 ± 1	6/6	6/6	6/6	48 ± 1
11 (no.1+4)	0/6	0/6	0/6	353-544								
12 (no.1+2)	0/6	0/6	0/6	347-687								
13 (no.1)	6/6	6/6	6/6	58 ± 1	6/6	6/6	6/6	48 ± 1				
20 (no.2+5)	0/6	0/6	0/6	361-518								
26 (no.1+3)	0/6	0/6	0/6	405-587								
U ⁴	6/6	6/6	6/6	48 ± 1	6/6	6/6	6/6	47 ± 1	6/6	6/6	6/6	46 ± 1

¹mouse identification number inoculated as pools.

²Positive for brain PrP^{res} by immunoblotting or histoblotting.

³For mice negative for disease clinical signs and for PrP^{res} accumulation, only the range of survival time is given.

⁴U: unfractionated material ([Additional File 1, supplementary Fig. 3](#)).

Table 3. Endpoint titration of LA19K and LA21K *fast* scrapie prions in transgenic mice expressing homotypic and heterotypic PrP

Dilution ¹	Survival time ² (n/n ₀) ³			
	LA19K		LA21K <i>fast</i>	
	Ovine PrP	Bovine PrP ⁴	Ovine PrP	Hamster PrP
10 ⁻⁰	<i>128 ± 2 (6/6)</i>	<i>196 ± 3 (6/6)</i>	<i>60 ± 2 (5/5)</i>	<i>153 ± 6 (6/6)</i>
10 ⁻¹	<i>151 ± 3 (6/6)</i>	<i>213 ± 5 (6/6)</i>	<i>64 ± 1 (5/5)</i>	<i>181 ± 11 (6/6)</i>
10 ⁻²	<i>167 ± 4 (6/6)</i>	<i>240 ± 5 (6/6)</i>	<i>71 ± 1 (5/5)</i>	<i>192; 230 (2/6)</i>
10 ⁻³	<i>188 ± 4 (6/6)</i>	<i>272 ± 19 (6/6)</i>	<i>79 ± 1 (6/6)</i>	<i>371-591 (0/6)</i>
10 ⁻⁴	<i>223 ± 15 (4/6)</i>	<i>361 ± 90 (4/6)</i>	<i>85 ± 1 (5/5)</i>	<i>399-518 (0/6)</i>
10 ⁻⁵	<i>245 (1/6)</i>		<i>99 ± 2 (5/5)</i>	<i>367-636 (0/6)</i>
10 ⁻⁶			<i>112 ± 2 (5/5)</i>	
10 ⁻⁷			<i>148 (1/5)</i>	

¹10% brain material used as 10⁻⁰ dilution.

²Days ± SE of the mean. For mice negative for disease clinical signs and for PrP^{res} accumulation, only the range of survival time is given.

³n/n₀: Number of mice with neurological disease and positive for PrP^{res} in the brain by immunoblotting/number of inoculated mice.

⁴tg110 line.

Data in italic are from [18].

Table 4. Summary of the transmission of SV-fractionated L-BSE prions to ovine PrP mice

Fractions	Total Attack rate	Clinical signs	PrP ^{res} detection ¹		Survival ² (days ± SEM)
			Brain	Spleen	
1	1/6	0/6	1/6	0/5	802
2	2/5	1/5	2/5	0/3	519 ; 739
3	0/5	0/5	0/5	0/4	532-711
4	1/6	1/6	1/6	0/3	496
6	1/6	0/6	1/6	0/2	472
8	3/6	2/6	3/6	0/2	542 ± 67
10	5/6	3/6	5/6	1/5	625 ± 64
12	6/6	4/6	6/6	1/4	575 ± 38
14	4/6	2/6	4/6	0/1	577 ± 76
16	2/6	0/6	2/6	1/4	530 ; 655
18	2/6	1/6	2/6	0/1	621 ; 681
20	0/6	0/6	0/6	0/3	406-877
22	2/6	1/6	2/6	0/3	479 ; 538
24	1/6	1/6	1/6	0/2	452
26	0/6	0/6	0/6	0/3	381-754
28	0/6	0/6	0/6	0/2	357-739
30	0/6	0/6	0/6	0/1	465-884
U³	9/9	9/9	8/8	8/8	423 ± 7

¹Positive for brain PrP^{res} by immunoblotting or histoblotting.

²For mice negative for disease clinical signs and for PrP^{res} accumulation, only the range of survival time is given. For positive mice, the mean survival time is derived from the individual survival times of clinical and subclinical mice.

³U: unfractionated material; data from [50,26] are in italic.

Table 5. Second passage of SV fractionated L-BSE prions in ovine PrP mice

Fractions (mouse no. ¹)	L-BSE	
	n/n₀²	Survival³
2 (no. 2)	7/7	162 ± 3
12 (no.3)	6/6	157 ± 3
18 (no. 3)	6/6	151 ± 1
24 (no.4)	6/6	193 ± 6

¹mouse number inoculated.

²n/n₀: Number of mice with neurological disease and positive for PrP^{res} in the brain by immunoblotting or histoblotting/number of inoculated mice.

³Mean survival time (days ± SE of the mean).